Na-induced variations in the structural, optical, and electrical properties of Cu(In,Ga)Se$_2$ thin films

Shogo Ishizuka,[1,a)] Akimasa Yamada,[1] Muhammad Monirul Islam,[2] Hajime Shibata,[1] Paul Fons,[1] Takeaki Sakurai,[2] Katsuhiro Akimoto,[2] and Shigeru Niki[1]

[1]*National Institute of Advanced Industrial Science and Technology (AIST), 1-1-1 Umezono, Tsukuba, Ibaraki 305-8568, Japan*
[2]*Institute of Applied Physics, University of Tsukuba, 1-1-1 Tennodai, Tsukuba, Ibaraki 305-8573, Japan*

The systematic variations in the structural, optical, and electrical properties of polycrystalline Cu(In,Ga)Se$_2$ (CIGS) thin films with Na doping level were investigated. Precise control of the Na concentration in CIGS films was demonstrated using alkali-silicate glass thin layers of various thicknesses deposited on substrates prior to CIGS growth. The CIGS grain size was observed to decrease with increasing Na concentration, although the surface morphology became smoother and exhibited a stronger (112) texture, which has been demonstrated consequence of larger grain size. The Ga composition gradient in the CIGS films was found to become large due to the presence of Na during growth, which in turn led to a decrease in the nominal band gap energy. Variations in the photoluminescence spectra and electrical properties suggested that the formation of an acceptor energy state, which may originate from O$_{Se}$ point defects, was enhanced in the presence of Na. This result suggests that not only Na, but also the presence of O in combination with Na contributes to the compensation of point defects and enhances *p*-type conductivity in CIGS films. © *2009 American Institute of Physics*. [DOI: 10.1063/1.3190528]

I. INTRODUCTION

Chalcopyrite Cu(In,Ga)Se$_2$ (CIGS) and related compounds are promising materials for optoelectronic devices such as solar cells,[1–3] light emitting diodes,[4] and image sensors.[5] Among these devices, solar cells fabricated based upon CIGS photoabsorber layers have been already put to practical use. Alkali metals, specifically Na, incorporated into CIGS absorber layers are widely known to have significantly beneficial effects that lead to enhanced CIGS-related photovoltaic cell efficiencies. The effect of Na includes an improvement in *p*-type conductivity due to an increase in the effective hole carrier density and improved open circuit voltage (V_{oc}) and fill factor for solar cells fabricated from Na-doped CIGS.[6,7] In addition to this, the effect of Na on the growth orientation of CIGS films results in an enhancement of (112) texture.[6,8,9] Numerous reports attempting to model the role of Na in CIGS films have been published, however, a definitive conclusion regarding the mechanism behind the Na effect has yet to be reached. Among the various Na effects, variations in the electrical properties have been well discussed. The observed improvement in V_{oc} has been proposed to originate from an increase in the effective acceptor density.[10] Na in polycrystalline CIGS films is considered to act on the grain boundaries rather than in the bulk.[11,12] The models proposed to account for the improved electrical properties in the literature are, for example, (i) the annihilation of the compensating antisite donor defect In$_{Cu}$ by Na (Na$_{Cu}$),[13] (ii) an increase in acceptor density due to the formation of

Na$_{In}$ antisite defects,[11,14] and (iii) the neutralization of donor-like Se vacancy defects by O atoms facilitated by the presence of Na.[15] Na substituting on a Cu site Na$_{Cu}$ results in the formation of a stable compound NaInSe$_2$, which has a larger band gap energy and in turn leads to a larger V_{oc} has been also proposed.[16] The correlation between the CIGS grain size and the presence of Na has been occasionally discussed. Both the enlargement[8,13,17] and decrease[12] of grain size have been reported. This may be due to the fact that the nature of the effects of Na on grain size depends on the CIGS growth method and the Na-doping process. In any case, the grain size of Na-doped CIGS films seems to have no critical role in solar cell performance.[18,19]

To carry out an accurate examination of the effect of Na on CIGS, the precise control of Na doping levels in CIGS is necessary. In our previous work, we have developed a technique using alkali-silicate glass thin layers (ASTL) of various thicknesses deposited on substrates prior to the Mo back contact layer deposition, which enables precise control of the Na doping level.[20] rf-magnetron sputter-deposited soda-lime glass thin films (SLGTF) were used as the ASTL. The Na incorporation in CIGS is speculated to be determined by the Na surface composition of the SLGTF and hence independent of SLGTF thickness. Our previous results have suggested, however, that this is not the case and that the thickness of the SLGTF plays an important role in determining the final Na concentration in CIGS films. Using this technique, enhanced cell efficiencies of flexible CIGS solar cells fabricated using various alkali-free substrates such as metal foils, ceramic sheets, and polyimide films have been demonstrated.[21,22] At the same time, the photovoltaic parameters of CIGS solar cells grown on alkali-free flexible sub-

a)Author to whom correspondence should be addressed. Electronic mail: shogo-ishizuka@aist.go.jp. Tel.: +81-29-861-3450. FAX: +81-29-861-5615.

strates showed systematic variations with the SLGTF thickness. Nonetheless, it was difficult to evaluate the relationship between the Na density and variations in CIGS film properties such as crystallography and optical and electrical properties using flexible substrates because of the presence of a nonflat surface, nontransparency, and the conductivity of the substrate. In the present work, the Na-doping level in CIGS grown on rigid alkali-free glass substrates was precisely controlled by the use of SLGTF of various thicknesses. Variations in the structural, optical, and electrical properties of CIGS films with increasing Na concentration were investigated.

II. EXPERIMENTAL

SLGTF layers ranging from 0 to 600 nm in thickness were deposited by rf-magnetron sputtering on alkali-free Corning 1737 alkaline earth boro-aluminosilicate (#1737) glass substrates without any intentional substrate heating. Although #1737 glass contains traces of alkali metals, the concentration of alkali impurities is much lower than that for SLG and here we consider #1737 as a nominally alkali-free substrate. CIGS thin films were grown by the three-stage process on SLGTF-coated #1737 substrates and on rigid SLG substrates for reference with and without Mo back contact layer deposition. The substrate thicknesses of #1737 and SLG were 0.7 mm. The CIGS growth chamber used in this study was designed to grow uniform films over an area of 100×100 cm^2. In a single growth run, CIGS films can thus be grown under nominally identical conditions on nine independent 30×30 cm^2 substrates. The simultaneous growth of multiple CIGS films avoids potential ambiguities that might arise from growth process variations. The growth temperature of the CIGS was kept constant at 350 °C during the first stage and raised to 550 °C during the second and third stages. The [Ga]/[In+Ga] and [Cu]/[In+Ga] composition ratios of the CIGS films determined by an electron probe microanalyzer were approximately 0.4 and 0.9, respectively. The thickness of the CIGS films was 1.8 μm.

The Na concentration in the CIGS films and the corresponding depth profiles of the constituent elements were studied by secondary ion mass spectroscopy (SIMS) measurements using Cs$^+$ as a primary ion with an acceleration voltage of 5 kV. The Na concentration was estimated from secondary ion intensities using a calibration based upon a known standard sample of Na ion-implanted CIGS. The surface morphology and grain size of the CIGS films were evaluated using scanning electron microscopy (SEM). The crystallographic structure was studied by x-ray diffraction (XRD) in the θ-2θ mode using Cu $K\alpha$ radiation. Photoluminescence (PL) spectra of CIGS films were measured at 1.4 K using Ar ion laser with an excitation wavelength of 514.5 nm using an InGaAs detector. Chemical bath deposition of CdS layers was performed after CIGS growth only for films intended for SIMS measurements to protect the film surface from compositional changes induced by exposure to atmosphere, whereas as grown CIGS films were used for SEM, XRD, PL, and other optical and electrical measurements.
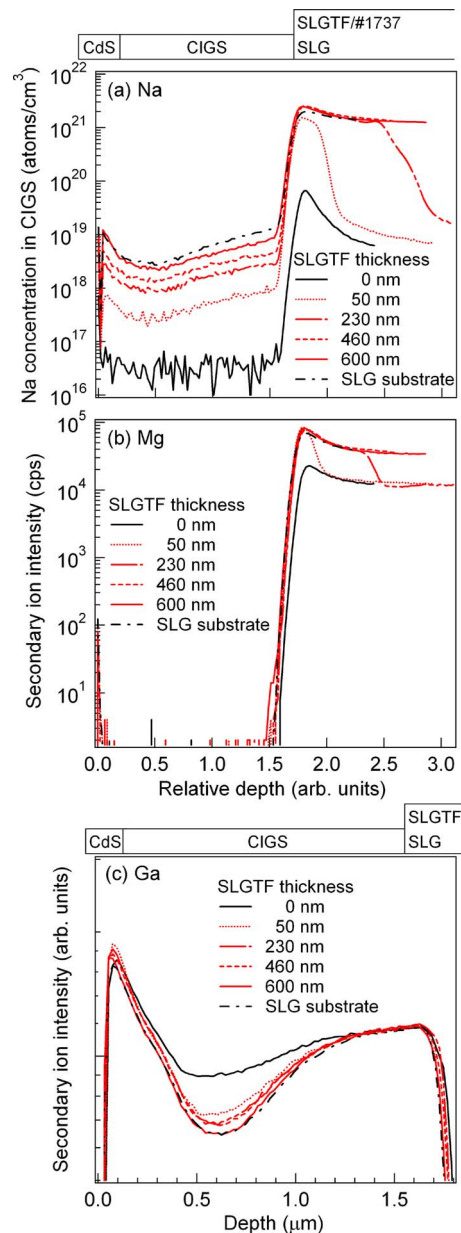

FIG. 1. (Color online) SIMS depth profiles of elemental Na (a), Mg (b), and Ga (c) distributions for CIGS films grown on SLGTF/#1737 and SLG substrates without Mo back contact layers. The secondary ion intensities of Ga have been normalized to the intensity at the CIGS/SLGTF interface. All CIGS films were grown in the same growth run.

III. RESULTS AND DISCUSSION

A. Variations in the structural properties of CIGS films with different SLGTF thicknesses

The variation in the Na concentration in CIGS films grown on #1737 and SLG substrates without Mo layers is shown in Fig. 1(a). The Na concentration was found to increase with increasing SLGTF thickness. This result implies that the Na concentration can be controlled by varying the thickness of the SLGTF deposited prior to CIGS growth. SLG consists chiefly of $Na_2O \cdot CaO \cdot 5SiO_2$ with a trace of metal oxides such as K_2O, Al_2O_3, and MgO.[23,24] When a Mo layer was inserted at the CIGS/SLGTF interface, diffusion of the multivalent metals Ca, Al, and Mg from SLGTF into the CIGS layer was almost completely blocked at the Mo layer

and only the diffusion of univalent alkali metals such as Na and K was observed.[21] The absence of a Mo layer may suggest a possibility of the diffusion of multivalent metal impurities into the CIGS layer as in the case of Zn diffusion into CIGS for cases where transparent ZnO films were used as back contact layers.[25] It was, in fact, found that incorporation of these multivalent metals from silicates was not observed regardless of the absence of Mo layers as can be seen for the case of Mg in Fig. 1(b). Similar results were observed for Ca and Al.

CIGS films grown by the three-stage process show unique Ga depth profiles as shown in Fig. 1(c), which is attributable to the absence of Ga source material during the second stage of the growth process and the low diffusion coefficient of Ga in CIGS. The Ga composition gradient was found to become steeper with increasing Na concentration, implying the presence of Na in growing CIGS film leads to a reduction in elemental interdiffusion of Ga. Similar trends have been observed with NaF coevaporation during the first stage of growth.[9]

Figure 2(a) shows the variation in the Na concentration in CIGS films grown on Mo (800 nm)-coated SLGTF/#1737 and SLG substrates. The SIMS depth profile of non-Mo-coated SLGTF(120 nm)/#1737 substrate is also shown for reference. Figures 2(b) and 2(c) show the Ga and In SIMS depth profiles for the same CIGS films. It should be noted that the amount of Na incorporated into CIGS depends on not only the SLGTF thickness but also the presence or absence of Mo layers and the substrate material. As shown in Figs. 1(a) and 2(a), the Na concentration in CIGS films grown without Mo layers was the order of $10^{17}-10^{18}$ cm^{-3}, whereas the Na concentration in CIGS films grown with Mo layers was the order of $10^{18}-10^{19}$ cm^{-3}. In addition to this, we have previously observed that the Na concentration in CIGS films grown on Mo/SLGTF/Ti-metal-foil substrates under the same growth conditions was the order of $10^{19}-10^{20}$ cm^{-3}.[20] The substrate surface of Mo-coated glass and metal foil can be considered to have higher thermal conductivity and lower heat capacity than that of a glass surface, thus, the thermal energy provided from the substrate surface and the actual growth temperature of CIGS films grown on metal can be higher even for the same growth run. Consequently, the Na diffusion into CIGS films grown on Mo-coated glass and metal substrates could be enhanced during CIGS growth. Figure 2(b) shows that the Ga gradient in CIGS films grown on Mo layers was small in comparison with films grown on non-Mo-coated glass substrates in spite of the high Na concentration in the CIGS films grown on Mo-coated substrates. This result is also attributable to thermodynamically enhanced elemental interdiffusion during growth. Another possible mechanism behind the increase in observed Na concentration in CIGS films grown on Mo-coated substrates is oxygen-induced diffusion. It has been proposed that as much as 10% of oxygen is present in the Mo layer and the Mo–O species can enhance transport of Na by forming Na-containing Mo oxides such as Na_2MoO_4.[7,15,26]

Variations in the grain size and surface texture of CIGS films as a function of SLGTF thickness are shown in Figs.
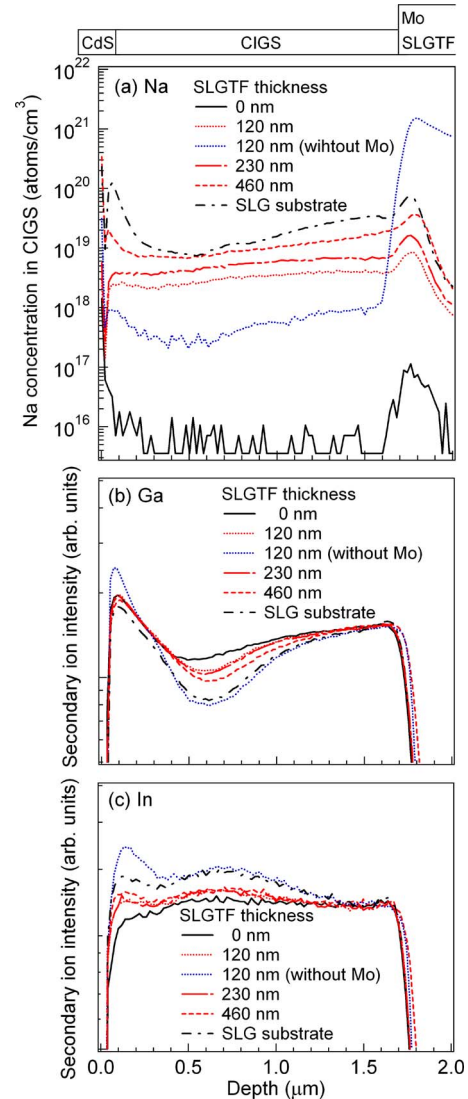

FIG. 2. (Color online) SIMS depth profiles of elemental Na (a), Ga (b), and In (c) distributions for CIGS films grown on Mo-coated glass substrates. The secondary ion intensities of Ga and In are displayed by normalizing the intensity at the CIGS/Mo interface. All CIGS films were grown in the same growth run.

3(a)–3(d). As can be seen in the cross sectional SEM images, CIGS films grown on SLGTF by the three stage process have exhibited decreased grain size with increasing SLGTF thickness, that is, with increasing Na concentration. This result is attributable to a reduction in the elemental interdiffusion occurring in the CIGS during growth as can be seen in the SIMS results. On the other hand, it should be noted that the surface texture became smooth with increasing Na concentration. This smooth texture may possibly lead to the mistaken impression of increased grain size, although a decrease in grain size can actually be found in the cross sectional SEM images. The smooth surface morphology is attributable to an enhancement in the (112) texture of the CIGS with increasing SLGTF thickness as shown in Fig. 4. However, CIGS films grown on (110)-oriented Mo layers exhibited an enhanced (220, 204) texture as shown in Fig. 5. As a consequence, CIGS films grown on Mo/SLG substrate exhibit relatively strong (220, 204) texture as shown in Fig. 4 even
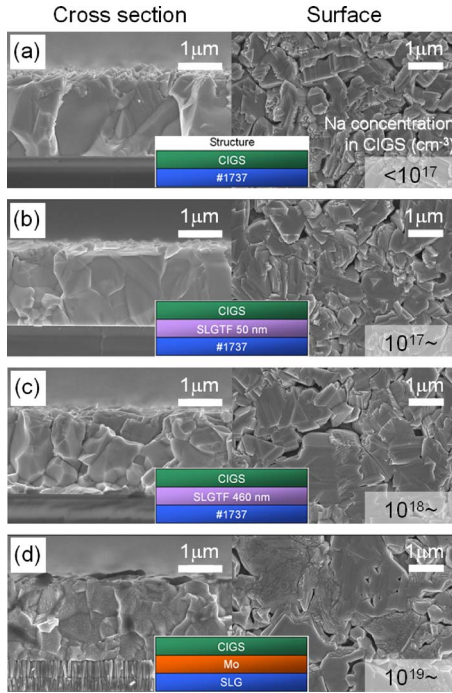
FIG. 3. (Color online) SEM images of the cross section and surfaces of CIGS films grown on #1737 (a), 50 nm-SLGTF/#1737 (b), 460 nm-SLGTF/#1737 (c), and Mo/SLG (d) substrates. The detailed Na concentration in the CIGS films can be found in Figs. 1(a) and 2(a).

though the CIGS film shows the highest Na concentration and the smoothest texture as can be seen in Figs. 2(a) and 3(d), respectively. This result, therefore, suggests the possibility of secondary phase formation of Na-related compounds such as Na(In,Ga)Se$_2$ on the grain surface[16] and also suggests that the surface appearance of CIGS films depends on not only the growth orientation.

B. Variations in the optical and electrical properties

Variations in the optical and electrical properties of CIGS thin films with increasing Na concentration were studied using a CIGS/SLGTF/#1737 structure without Mo back contact layers. Figure 6 shows $(\alpha h\upsilon)^2$ as a function of $h\upsilon$,
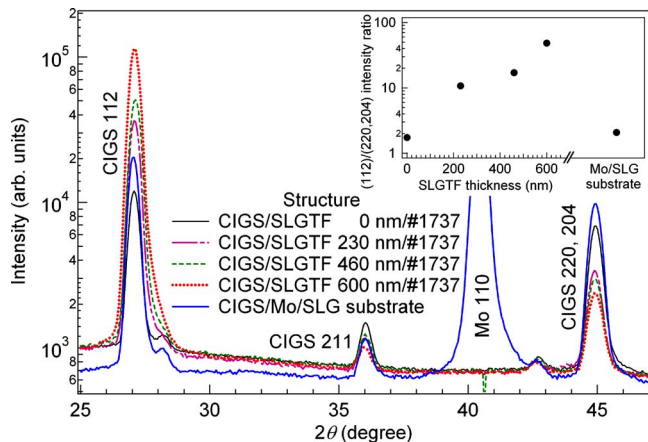

FIG. 4. (Color online) Variations in the XRD patterns of CIGS films with various SLGTF thicknesses. The XRD pattern of a CIGS film grown on a Mo/SLG substrate is shown for reference. The inset figure shows the (112)/(220, 204) intensity ratio of the XRD patterns.
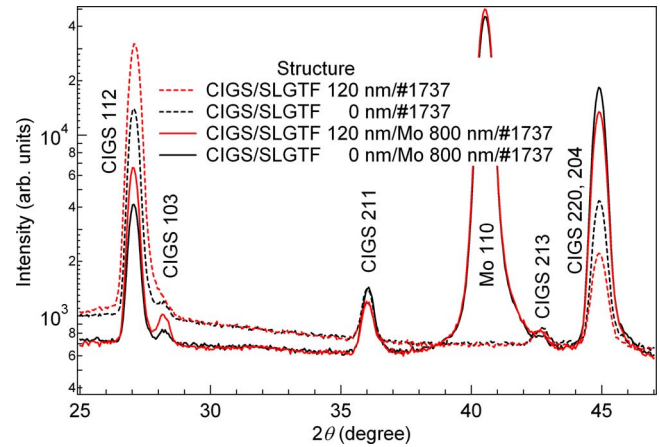

FIG. 5. (Color online) XRD patterns of CIGS films grown on #1737 substrates with and without SLGTF and Mo back contact layers.

where α is the absorption coefficient and $h\upsilon$ is the photon energy. As indicated with an arrow, the gradient of the curve above the absorption threshold becomes smaller with increasing Na concentration. This result is attributable to increased spatial inhomogeneity of the band-gap energy (E_g). As shown in Fig. 1(c), the presence of Na in the CIGS leads to a reduction in interdiffusion during growth, resulting in a steeper Ga composition gradient. The distribution profile of Ga relative to that of In in CIGS films can be nominally considered as a profile of the variation in the conduction band minimum in the CIGS. It is, therefore, suggested that such an extended inhomogeneity in the Ga distribution amplifies the variation of E_g in the CIGS resulting in a decrease in the nominal E_g. Consequently, the decreased E_g enhances the absorption in the long wavelength region as can be seen in the external quantum efficiency curves of the corresponding solar cells.[20,21]

Figure 7 shows PL spectra for CIGS films grown on SLGTF/#1737 substrates. The PL emission intensity was found to increase in the low photon energy region with increasing SLGTF thickness. The nominal E_g of the CIGS can be estimated to be 1.20–1.25 eV from the group III elemental composition ratio ([Ga]/[In+Ga]$\sim$0.4) and the absorption threshold shown in Fig. 6. The PL emission peaks observed around 1.0–1.2 eV consist chiefly of two prominent emis-
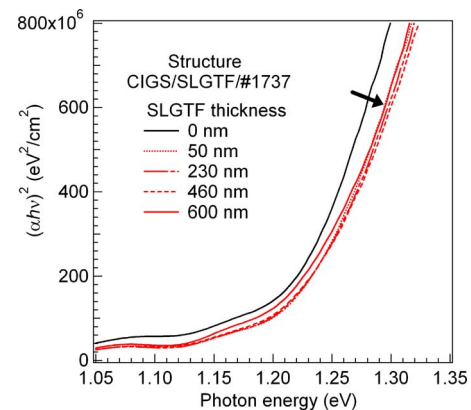

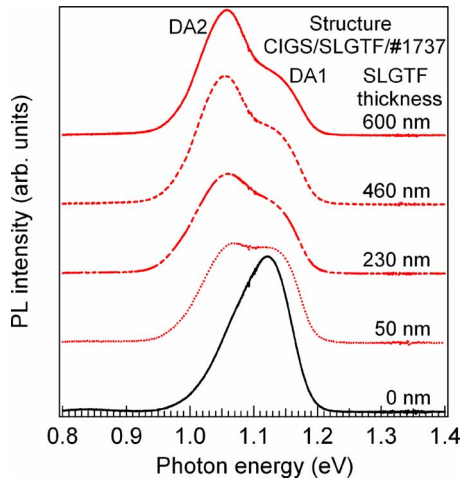FIG. 6. (Color online) Relation between $(\alpha h\upsilon)^2$ and $h\upsilon$ for CIGS films grown on SLGTF/#1737 substrates.

FIG. 7. (Color online) Variation in the PL spectra of CIGS films grown on SLGTF/#1737 substrates with SLGTF thickness.

FIG. 8. Resistivity variations in CIGS films grown on #1737 glass substrates for various thicknesses with SLGTF layers.

sions at 1.05–1.07 eV (DA2) and 1.12–1.14 eV (DA1) and are attributable to donor-acceptor pair (DAP) luminescence. We observed a blue shift of these emission peaks with increasing excitation power. Taking the E_g of 1.20–1.25 eV of the CIGS films into account, these DAP emissions can be considered to originate from relatively shallow acceptor and donor energy levels such as Cu vacancy (V_{Cu}) acceptors ($E_v + 0.03$ eV) with Se vacancy (V_{Se}) donors ($E_c - 0.08$ eV) or Cu interstitial (Cu_i) donors ($E_c - 0.20$ eV). Here the stated acceptor and donor levels are the reported values based upon calculations of CuInSe$_2$ in the literature,[27,28] and may be close to the values for CIGS, where E_v is the valence band maximum and E_c is the conduction band minimum. From the viewpoint of the stoichiometric deviation of the films toward Cu-poor composition ([Cu]/[In+Ga] $\sim$ 0.8), V_{Cu} and In$_{Cu}$ defects likely occur followed by the formation of electrically neutral $2V_{Cu}^- + In_{Cu}^{2+}$ complex defects.[29] However, the In$_{Cu}$ (0/+) donor level in CuInSe$_2$ is expected to create a relatively deep level ($E_c - 0.25$ eV),[27] therefore, if In$_{Cu}$ defect-related DAP emissions appear in the PL spectra, the emission peak should be observed below 1.0 eV. As shown in Fig. 7, however, no emission peaks below 1.0 eV were observed. This result may imply that the In$_{Cu}$ defect-related transitions are, even though this In$_{Cu}$ point defect is present, nonradiative and the evaluation of the annihilation of the compensating antisite In$_{Cu}$ donor defects by Na using PL measurements is difficult. On the other hand, the PL emissions above 1.0 eV showed obvious variations. The emission intensities of DA1 decreased and DA2 increased with increasing SLGTF thickness, that is, with increasing Na concentration. The decreased intensity of the DA1 emissions, which likely originates from a DAP of V_{Cu}-V_{Se} taking into account the peak position, may be due to the compensation of V_{Cu} with Na (Na$_{Cu}$) or the compensation of V_{Se} with O facilitated by the presence of Na (O$_{Se}$). The O$_{Se}$ has been reported to form an acceptor level of 0.12–0.14 eV above the E_v.[15,30] Thus, the increased emission intensity of DA2 is, at the same time, likely attributable to an increase in the O$_{Se}$ acceptor concentration. We have observed an increase in the oxygen concentration 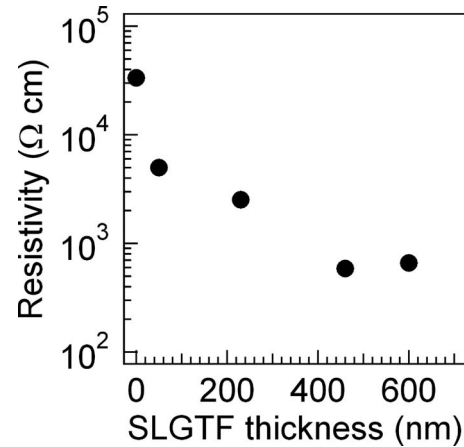in CIGS with increasing Na concentration. A similar trend in the PL emissions seen in Fig. 7 has been observed with the air annealing of CuInSe$_2$ films,[31] which also supports a correlation between the increase in DA2 emission intensity and the formation of O$_{Se}$. Cu$_i$-related defects such as V_{Cu}-Cu$_i$ are also possible origins of the broad DA2 emission. It has been proposed that Na reacts strongly with CuInSe$_2$ and leads to the breaking of Cu–Se bonds at grain boundaries. Na$^+$ ions on the surface then drive Cu$^+$ ions into the bulk by the induced electric field and lead to a reduction in the Cu 3d contribution to the valence band density of states.[11,32] Thus, the replacement of Cu by Na causes a reduction in the electronic charge resulting in an enhancement of p-type conductivity and a simultaneous formation of interstitial defect of Cu$_i$ is expected. However, the energy of the donor state created by the Cu$_i$ is expected to be around $E_c - 0.20$ eV, thus this donor state is slightly too deep to contribute to the DA2 emission. Therefore, the O$_{Se}$ acceptor model seems to be more reasonable. It should be noted that the DA2 emission intensity decreased again in highly Na-doped CIGS films grown on SLG and Mo/SLG substrates. This result is attributable to an increase in defect density which acts as a non-radiative recombination center due to excessive incorporation of Na or O impurities.

Figure 8 shows the decrease in the resistivity observed with increasing Na concentration for films grown on SLGTF/#1737 substrates. This trend is similar to typical Na effects reported in the literature.[13,33,34] Numerous models have been proposed thus far to account for the mechanism behind the increase in the hole carrier density induced by the presence of Na in CIGS.[11,13–16,30–32] As mentioned above, these models include, for example, point defect acceptors such as Na$_{Cu}$, Na$_{In}$, and O$_{Se}$ acting on/in the CIGS grains, and/or passivation of grain boundaries by the formation of In–O bonds. Among these explanations, the Na$_{Cu}$ and O$_{Se}$ models seem to be most consistent with the result in the present work. The Na$_{Cu}$ defect, which leads to the annihilation of the antisite donor defect In$_{Cu}$ and/or the formation of the NaInSe$_2$ phase, may explain the improved p-type conductivity and the variation of the surface morphology of the CIGS films. Although Wei *et al.*[16] proposed that O$_{Se}$ creates deep levels at $E_v + 0.55$ eV (-/0) and $E_v + 0.67$ eV (2-/-) in the bulk rather than shallow acceptor levels at 0.12–0.14 eV above the E_v as

mentioned above, they have also suggested that O_{Se} acceptor levels are expected to be shallower near the surface where covalency is reduced. It is, therefore, suggested that O atoms accompanied by Na at CIGS grain boundaries compensate V_{Se} by forming O_{Se} and the shallow O_{Se} acceptor level contributes to an increase in the DA2 emission in the PL spectra and enhances *p*-type conductivity. The decreased grain size of films results in an increase in grain boundaries in films. Therefore, the model of O_{Se} acceptors, which act at grain surfaces rather than in the bulk is consistent with the result observed in the relationship between decreased grain size and increased DA2 emission intensity with increasing Na concentration. It should be noted, however, that this result does not imply the impossibility of Na effects (including O effects) acting in the bulk crystal. The presence of Na or associated O in CIGS films during growth was obviously found to affect the growth mode of CIGS as observed in the variations in Ga depth profiles and crystal texture, and thus may lead to the formation of Na- and O-induced point defects in bulk CIGS as well.

In this work, only the effects of Na and O incorporated into CIGS films from SLGTF were proposed to account for the variations observed in the structural, optical, and electrical properties of CIGS films. Further investigation of the influence of Na on CIGS interfaces and *pn*-junction formation taking into account the presence of *n*-type buffer layers such as CdS, ZnS(O,OH), and In_2S_3 may bring further understanding of the detailed mechanisms behind the enhancement of CIGS solar cell efficiency with Na incorporation.

IV. SUMMARY

Variations in the structural, optical, and electrical properties of CIGS films in which the Na doping level was controlled with the use of SLGTF of various thicknesses deposited on substrates prior to CIGS growth was studied. The Na doping level in CIGS films was found to depend on not only the SLGTF thickness, but also the presence of Mo back contact layers and the substrate material. The Ga composition gradient in CIGS films became larger and the grain size decreased with increasing Na concentration. This structural variation affects the optical properties of CIGS and leads to a decrease in the nominal E_g. An enhanced (112) texture was observed with increasing SLGTF thickness thus Na concentration, although CIGS films grown on (110)-oriented Mo layers retained (220, 204) texture in spite of the high Na concentration and the smooth surface morphology. Variations in the PL spectra and electrical properties suggested the importance of O facilitated by the presence of Na in CIGS films.

ACKNOWLEDGMENTS

[1]S. Wagner, J. L. Shay, P. Migliorato, and H. M. Kasper, Appl. Phys. Lett. **25**, 434 (1974).

[2]A. M. Gabor, J. R. Tuttle, D. S. Albin, M. A. Contreras, R. Noufi, and A. M. Hermann, Appl. Phys. Lett. **65**, 198 (1994).

[3]I. Repins, M. A. Contreras, B. Egaas, C. DeHart, J. Scharf, C. L. Perkins, B. To, and R. Noufi, Prog. Photovoltaics **16**, 235 (2008).

[4]S. F. Chichibu, T. Ohmori, N. Shibata, T. Koyama, and T. Onuma, Appl. Phys. Lett. **85**, 4403 (2004).

[5]K. Miyazaki, O. Matsushima, M. Moriwake, H. Takasu, S. Ishizuka, K. Sakurai, A. Yamada, and S. Niki, Thin Solid Films **517**, 2392 (2009).

[6]J. Hedström, H. Ohlsén, M. Bodegård, A. Kylner, L. Stolt, D. Hariskos, M. Ruckh, and H. W. Schock, *Conference Record of the 23rd IEEE Photovoltaic Specialists Conference*, Louisville (IEEE, New York, 1993), p. 364.

[7]M. Ruckh, D. Schmid, M. Kaiser, R. Schäffler, T. Walter, and H. W. Schock, *Conference Record of the 1994 IEEE First World Conference on Photovoltaic Energy Conversion*, Waikoloa (IEEE, New York, 1994), p. 156.

[8]M. Bodegård, K. Granath, and L. Stolt, Thin Solid Films **361-362**, 9 (2000).

[9]D. Rudmann, G. Bilger, M. Kaelin, F.-J. Haug, H. Zogg, and A. N. Tiwari, Thin Solid Films **431-432**, 37 (2003).

[10]T. Nakada, D. Iga, H. Ohba, and A. Kunioka, Jpn. J. Appl. Phys., Part 1 **36**, 732 (1997).

[11]D. W. Niles, M. Al-Jassim, and K. Ramanathan, J. Vac. Sci. Technol. A **17**, 291 (1999).

[12]D. Rudmann, A. F. da Cunha, M. Kaelin, F. Kurdesau, H. Zogg, A. N. Tiwari, and G. Bilger, Appl. Phys. Lett. **84**, 1129 (2004).

[13]M. A. Contreras, B. Egaas, P. Dippo, J. Webb, J. Granata, K. Ramanathan, S. Asher, A. Swartzlander, and R. Noufi, *Conference Record of the 26th IEEE Photovoltaic Specialists Conference*, Anaheim (IEEE, New York, 1997), p. 359.

[14]D. W. Niles, K. Ramanathan, F. Hasoon, R. Noufi, B. J. Tielsch, and J. E. Fulghum, J. Vac. Sci. Technol. A **15**, 3044 (1997).

[15]L. Kronik, D. Cahen, and H. W. Schock, Adv. Mater. (Weinheim, Ger.) **10**, 31 (1998).

[16]S.-H. Wei, S. B. Zhang, and A. Zunger, J. Appl. Phys. **85**, 7214 (1999).

[17]V. Probst, J. Rimmasch, W. Riedl, W. Stetter, J. Holz, H. Harms, F. Karg, and H. W. Schock, *Conference Record of the 1994 IEEE First World Conference on Photovoltaic Energy Conversion*, Waikoloa (IEEE, New York, 1994), p. 144.

[18]W. N. Shafarman and J. Zhu, Thin Solid Films **361-362**, 473 (2000).

[19]S. Ishizuka, H. Shibata, A. Yamada, P. Fons, K. Sakurai, K. Matsubara, and S. Niki, Appl. Phys. Lett. **91**, 041902 (2007).

[20]S. Ishizuka, A. Yamada, K. Matsubara, P. Fons, K. Sakurai, and S. Niki, Appl. Phys. Lett. **93**, 124105 (2008).

[21]S. Ishizuka, A. Yamada, P. Fons, and S. Niki, J. Renewable Sustainable Energy **1**, 013102 (2009).

[22]S. Ishizuka, H. Hommoto, N. Kido, K. Hashimoto, A. Yamada, and S. Niki, Appl. Phys. Express **1**, 092303 (2008).

[23]G. N. Greaves, A. Fontaine, P. Lagarde, D. Raoux, and S. J. Gurman, Nature (London) **293**, 611 (1981).

[24]D. F. Dawson-Elli, C. B. Moore, R. R. Gay, and C. L. Jensen, *Conference Record of the 1994 IEEE First World Conference on Photovoltaic Energy Conversion*, Waikoloa (IEEE, New York, 1994), p. 152.

[25]K. Sakurai, M. Yonemura, S. Ishizuka, K. Matsubara, A. Yamada, S. Niki, M. Sugiyama, and H. Nakanishi, *Proceedings of the 22nd European Photovoltaic Solar Energy Conference and Exhibition*, Milan (WIP, Munich, 2007), p. 1867.

[26]A. Rockett, M. Bodegård, K. Granath, and L. Stolt, *Conference Record of the 25th IEEE Photovoltaic Specialists Conference*, Washington, D.C. (IEEE, New York, 1996), p. 985.

[27]S.-H. Wei, S. B. Zhang, and A. Zunger, Appl. Phys. Lett. **72**, 3199 (1998).

[28]S. M. Wasim, Sol. Cells **16**, 289 (1986).

[29]S. B. Zhang, S.-H. Wei, A. Zunger, and H. Katayama-Yoshida, Phys. Rev. B **57**, 9642 (1998).

[30]G. Dagan, F. Abou-Elfotouh, D. J. Dunlavy, R. J. Matson, and D. Cahen, Chem. Mater. **2**, 286 (1990).

[31]K. Kushiya, H. Hakuma, H. Sano, A. Yamada, and M. Konagai, Sol. Energy Mater. Sol. Cells **35**, 223 (1994).

[32]A. Klein, T. Löher, C. Pettenkofer, and W. Jaegermann, J. Appl. Phys. **80**, 5039 (1996).

[33]R. Kimura, T. Mouri, T. Nakada, S. Niki, Y. Lacroix, T. Matsuzawa, K. Takahashi, and A. Kunioka, Jpn. J. Appl. Phys., Part 2 **38**, L289 (1999).

[34]N. Kohara, T. Negami, M. Nishitani, Y. Hashimoto, and T. Wada, Appl. Phys. Lett. **71**, 835 (1997).